Breaking of thunderstorm-generated gravity waves as a source of short-period ducted waves at mesopause altitudes

Jonathan B. Snively and Victor P. Pasko

CSSL Laboratory, The Pennsylvania State University, University Park, Pennsylvania, USA

Received 16 August 2003; revised 2 October 2003; accepted 7 November 2003; published 19 December 2003.

[1] Numerical simulation results indicate that the breaking of atmospheric gravity waves generated by tropospheric convection can excite short-period secondary waves, which are trapped in the lower thermospheric duct and which closely resemble quasi-monochromatic structures commonly observed in airglow imaging experiments. *INDEX TERMS:* 3314 Meteorology and Atmospheric Dynamics: Convective processes; 3332 Meteorology and Atmospheric Dynamics: Mesospheric dynamics; 3334 Meteorology and Atmospheric Dynamics: Middle atmosphere dynamics (0341, 0342); 3369 Meteorology and Atmospheric Dynamics: Thermospheric dynamics (0358); 3384 Meteorology and Atmospheric Dynamics: Waves and tides. **Citation:** Snively, J. B., and V. P. Pasko, Breaking of thunderstorm-generated gravity waves as a source of short-period ducted waves at mesopause altitudes, *Geophys. Res. Lett.*, *30*(24), 2254, doi:10.1029/2003GL018436, 2003.

1. Introduction

[2] It is well established that mechanical oscillations of air due to penetrative convection at thundercloud tops can lead to upward launching of gravity waves (GWs) [e.g., *Pierce and Coroniti*, 1966; *Stull*, 1976; *Fovell et al.*, 1992; *Alexander et al.*, 1995; *Piani et al.*, 2000; *Horinouchi et al.*, 2002], which are observed in different parts of the atmosphere above thunderstorms [e.g., *Larsen et al.*, 1982; *Taylor and Hapgood*, 1988; *Dewan et al.*, 1998; *Sentman et al.*, 2003].

[3] Airglow imaging reveals that quasi-monochromatic, small-scale, GWs frequently propagate through the upper mesosphere and lower thermosphere. Waves with periods of $5 \leq \tau \leq 8$ min with horizontal wavelengths (λ_x) on the order of a few tens of km have been observed [*Taylor et al.*, 1995; *Walterscheid et al.*, 1999; *Hecht et al.*, 2001]; it is believed that these waves may be guided or trapped by a thermal duct [e.g., *Walterscheid et al.*, 1999]. Many of these GWs have been traced to thunderstorm activity thousands of km away from the point of observation, implying ducted propagation. However, these GWs are evanescent in regions of atmosphere where their frequency exceeds the local Brunt-Väisälä frequency. It is therefore improbable that the observed waves with short periods $\tau \simeq 5$ min would be able to propagate freely from a tropospheric convective source to a duct at airglow altitudes, given the thick evanescent region separating the stratosphere and lower thermosphere (see Figure 1).

[4] *Walterscheid et al.* [2001] applied a convective source at tropospheric altitudes to study the generation and propagation of short period waves in a realistic atmosphere using a cylindrically-symmetric, two-dimensional (2-D) model. Results clearly indicated some degree of coupling between ducts, where waves first propagated into a stratospheric duct before transferring vertically into the lower thermospheric duct. In all simulation results presented, guided small-scale waves were excited in the lower thermosphere. The interaction between ducts resembles the ''kissing'' modes described in past studies [e.g., *Fritts and Yuan*, 1989]. These simulated waves were also consistent with past observations of small-scale GWs [e.g., *Walterscheid et al.*, 1999; *Hecht et al.*, 2001]. This coupling is likely to be an effective linear source of high-altitude, short-period, ducted GWs.

[5] It is possible for GWs of stronger magnitude to be generated by a realistic thunderstorm, particularly in the case of squall line sources where wave magnitude does not strongly decrease with radial distance from the source [e.g., *Alexander et al.*, 1995]; it can be expected that many of these waves will break at some altitude near the mesopause.

[6] Recent studies of nonlinear wave breaking in 2-D reveal that coherently propagating secondary waves may be excited in the breaking region. *Franke and Robinson* [1999] demonstrated the excitation of both acoustic and GW modes during the breaking of short-period GWs. The secondary waves radiated from the breaking region had characteristic frequencies and horizontal wavenumbers that were integer multiples of the source waves, with perturbation magnitudes consecutively weaker for each higher mode. Similar results were presented by *Zhou et al.* [2002], who studied the generation of secondary waves during breaking for a broadband convective source rather than an ideal, quasi-monochromatic source. As a means to model the effects of breaking, *Vadas et al.* [2003] treated the generation of secondary waves as a linear response to the small-scale convection that would be present in the breaking region. *Vadas et al.* [2003] noted that these secondary waves may become ducted at certain altitudes.

[7] GW breaking at airglow altitudes has been observed and recorded in past studies. *Yamada et al.* [2001] observed from OH airglow data a propagating small-scale ($\lambda_x \simeq$ 27 km) wave with short-period ($\tau \simeq 5.6$ min) breaking down into turbulence. Breakdown of larger waves at airglow heights has also been observed [*Hecht et al.*, 1997] and studied [*Fritts et al.*, 1997]; such long-period wave breaking is able to excite a broad range of GWs, thus producing a superposition of propagating smaller-scale waves and instability structures.

[8] *Hecht et al.* [2001] and *Walterscheid et al.* [1999, 2001] demonstrated how short period ($5 \leq \tau \leq 8$ min) waves can be trapped in a thermal (or combined thermal-Doppler) duct at mesopause altitudes. However, this

0094-8276/03/2003GL018436$05.00

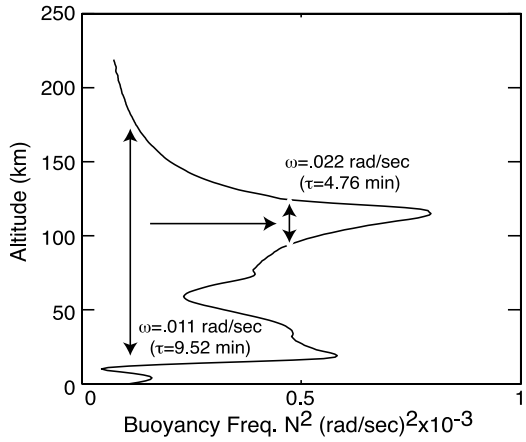

Figure 1. Altitude profile of the squared Brunt-Väisälä frequency used in studies reported in this paper. The vertical arrows show predicted altitudes of reflection and ducting of primary wave with ω = 0.011 rad/sec (τ = 9.52 min) and secondary wave with ω = 0.022 rad/sec (τ = 4.76 min) generated by the primary wave breaking.

requires somewhat special conditions to allow these waves to first enter the duct without too much loss of wave energy. Given the predominance of longer-period waves ($10 \leq \tau \leq 16$ min) being generated by tropospheric convection (consistent with buoyancy properties of the upper troposphere [*Pierce and Coroniti*, 1966]), and the ability of these waves to freely propagate up to mesopause altitudes, we can formulate an alternate explanation. If a wave with period of 10 to 16 min were to break at some altitude near mesopause, it is likely that some wave energy will be transferred to harmonic secondary waves, with wavenumber and frequency of $\sim 2k_x$ and $\sim 2\omega$ of the source [*Franke and Robinson*, 1999]. These secondary waves would thus have periods $\sim$5 to 8 min, and would be stable in the Brunt-Väisälä frequency maximum comprising the lower thermospheric duct (Figure 1). It can thus be predicted that the breaking of convectively generated GWs originating from the troposphere may be able to excite high-altitude, short-period, ducted GWs. The study of this process by means of high-resolution numerical simulation is the goal of the present paper.

2. Model Formulation

[9] The employed numerical model is 2-D, nonlinear, inviscid, compressible, and non-rotating. It is based on a flux limited, finite volume method developed by *LeVeque* [1997] and implemented in the CLAWPACK software package solving the inviscid Euler equations in conservative form for a nonlinear, ideal gas [http://www.amath.washington.edu/claw]. The force of gravity is included using the flux-differencing "f-wave" method [*LeVeque*, 2002, p. 399]. The scheme is shock-capturing and supports discontinuous solutions and nonlinearities without instability. Although we consider subsonic flow, this added stability allows us to explore wave growth and breaking without the explicit application of diffusion.

[10] The simulation domain is a 2-D Cartesian space, with the x-axis parallel to the surface of the ground and the z-axis directed vertically and denoting altitude. The domain extends from ground to an altitude of 220 km, and has a horizontal dimension of 1200 km with uniform vertical and horizontal grid resolutions Δ_z = 1 km and Δ_x = 1.5 km, respectively. The source of the GWs is positioned at x_o = 450 km and z_o = 12 km (i.e., 450 km from the left boundary of the simulation domain and at 12 km altitude). The source is a mechanical standing-wave oscillator providing a vertical force at a chosen frequency(ω) and horizontal wavenumber (k_x) of the form $\sim \exp[-(x - x_o)^2/2\sigma_x^2 - (z - z_o)^2/2\sigma_z^2 - (t - t_o)^2/2\sigma_t^2] \cos[k_x x] \cos[\omega t]$, where σ_x and σ_z are the Gaussian envelope's horizontal and vertical half-widths, respectively, and σ_t is the temporal Gaussian half-width; the position given by x_o, z_o, and t_o corresponds with the source maximum in space and time. The sinusoidal forcing is therefore turned on smoothly in time using a Gaussian transient, thus providing broadband forcing centered around the desired frequency; the breadth of the spectrum can be modified by changing the packet's temporal width with respect to the period of oscillation. The source approximates the oscillations arising from convection that occur above a realistic thunderstorm [e.g., *Pierce and Coroniti*, 1966]. Similar oscillatory sources were used by *Fovell et al.* [1992].

[11] Both lateral and vertical boundaries are equipped with sponge layers as a means to control wave reflections. The sponge layers apply Rayleigh friction damping to reduce the outgoing wave magnitude [e.g., *Franke and Robinson*, 1999]. The simulation boundaries are thus approximately "open" for both gravity and acoustic wave modes.

[12] We consider an atmosphere with two distinct thermal ducts; a stratospheric duct at $\sim$30 km and a lower thermospheric duct at an altitude of $\sim$110 km (Figure 1). The model profile (Figure 1) approximately matches that used by *Walterscheid et al.* [2001]; it is obtained for June 15, 2001, at noon LT, for a geographical lat. $-$11 and long. 131 using data from the MSIS-E-90 model [*Hedin*, 1991, http://nssdc.gsfc.nasa.gov/space/model/atmos/msise.html].

[13] Simulation parameters are chosen so that the waves generated by the tropospheric source will break at mesopause altitudes. The source wave frequency is chosen to coincide with the Brunt-Väisälä frequency of the upper troposphere, and is sufficiently low such that the primary waves will not be reflected prior to breaking. If the source magnitude were lower, the waves would be reflected at some altitude near the upper sponge layer and would become weakly trapped between the thermosphere and the upper troposphere.

[14] We do not include thermal, eddy, or molecular diffusion; their effects are minimal for the time scales of interest and would not significantly change the results. We also ignore the effects of winds. Possible implications of wind effects will be discussed in section 4.

3. Results

[15] Figure 2 shows results of model calculations for source parameters ω = 0.011 rad/sec, k_x = 0.00011 rad/m, σ_x = 30 km, σ_z = 4 km, σ_x = 10 min, and forcing velocity max($\tilde{v}_z$) = 0.33 m/s. The quantity presented in Figure 2 is the normalized vertical velocity $w_z = (\rho/\rho_o)^{1/2} v_z$, where ρ_o and ρ are atmospheric neutral densities at the ground level

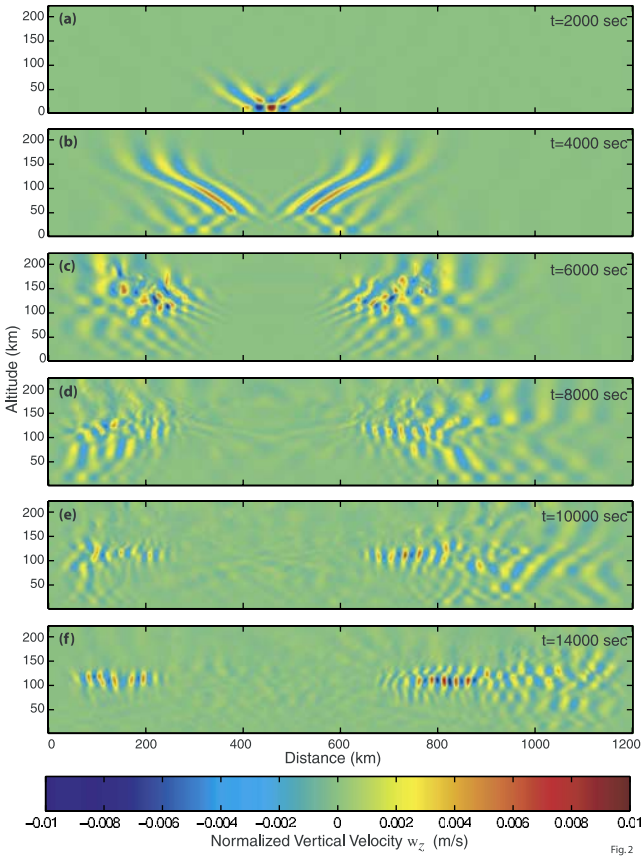

Figure 2. The normalized velocity w_z at selected instants of time.

and at an altitude z, respectively. The tropospheric source is applied from ~800 to ~3200 sec (Figure 2a). This results in a freely-propagating GW, which grows in magnitude as it propagates to higher altitudes (Figure 2b). The wave spectrum (Figure 3) is initially centered around the source ω and k_x. As the wave propagates vertically and the velocity perturbation magnitude increases, the wave becomes increasingly nonlinear and approaches instability. By the 6000 sec frame, shown in Figure 2c, wave breaking has begun. The initial product of breaking is turbulence and a broadened spectrum including high-frequency and short-wavelength components not present in the source wave (Figure 3). Figure 2d demonstrates that, by 8000 sec into the simulation, coherent structures are forming in the region of the lower thermospheric duct. As the simulation evolves, these small-scale waves become a dominant feature of the lower thermosphere and upper mesosphere. As shown in Figure 2f, after 14000 sec this new wave mode is trapped in the lower thermospheric duct.

[16] Figure 3a indicates that inside of the lower thermospheric duct at 110 km altitude and at a horizontal distance of 180 km from the source the primary wave is clearly observed until 5000 sec into the simulation; the wave then breaks and energy is transferred from the low-frequency primary wave to secondary waves with higher frequency. The measured frequency appears to be slightly higher than the expected double frequency of 0.022 rad/sec [e.g., *Franke and Robinson*, 1999]; this can be attributed to the broadband nature of the source along with the characteristics of the duct, which would selectively capture wave modes that conform well to its structure. The high-frequency spectral peak in Figure 3a is visible until the secondary waves propagate past the 180 km measurement point. Similarly, at 225 km from the source (Figure 3b), the presence of the secondary wave can be seen until the time that the wave has passed the measurement point.

[17] Figure 3c illustrates the k_x spectrum at z = 110 km for the horizontal region of 525 to 825 km (75 km to 375 km from the source) as a function of time. The first waves to reach the altitude of the duct have k_x approximately consistent with the source k_x of 0.00011 rad/m. During breaking, the spectrum broadens to include higher k_x components, specifically the first harmonic of the excitation wave, with k_x approximately twice that of the source [e.g., *Franke and Robinson*, 1999]. The new, small-scale, short-period structure evolves to become a dominant feature in the spectrum.

4. Discussion

[18] For the simulation results presented in this paper, the source has a period of 9.52 min, such that the secondary waves have a period near 4.76 min. These secondary waves are necessarily ducted, as they are reflected by the upper and lower boundaries of the lower thermospheric duct (Figure 1). The secondary waves will remain stable if their magnitude is less than that of the primary wave and if the mean flow acceleration resulting from breaking is small enough not to induce further breakdown. The duct will confine the secondary waves such that they cannot propagate higher to the point that they would break. If the waves conform well to the characteristics of the duct, they will be able to propagate long distances as fully-ducted wave modes. In our simulated results (section 3), the trapped secondary waves propagate horizontally with minimal loss, suggesting that the ducting is effective and that the secondary waves are stable at the altitude of the duct. We emphasize that results similar to those presented in section 3 can be obtained for a fairly broad range of parameters and the discussed physical mechanism is not sensitive to specific numerical values given in section 3.

[19] The principal results reported in this paper are not sensitive to specific model geometry; however, we note that our two-dimensional Cartesian model is more consistent with a squall line [e.g., *Alexander et al.*, 1995] than an

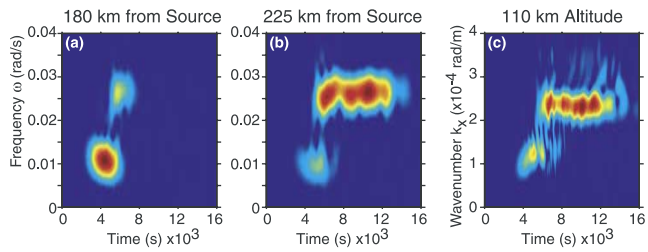

Figure 3. (a) and (b) Dynamic frequency spectra corresponding to results presented in Figure 2 taken at an altitude of 110 km (i.e., inside of the lower thermospheric duct) and horizontal distances of 180 km and 225 km from source, respectively; (c) horizontal wavenumber k_x spectrum vs. time taken at 110 km altitude for the 525 to 825 km horizontal region of the simulation domain.

isolated, convective source [e.g., *Taylor and Hapgood*, 1988; *Dewan et al.*, 1998; *Sentman et al.*, 2003]. It therefore exhibits a slower geometrically-related decrease in wave magnitude with respect to the horizontal distance from the source, in contrast with a cylindrically axisymmetric model [e.g., *Walterscheid et al.*, 2001]. The Cartesian model does, however, allow for the future inclusion of wind flow.

[20] Winds are an unavoidable feature of a realistic atmosphere. Waves propagating in the direction of the wind flow will be subject to Doppler shifting effects and possible critical level dissipation [*Booker and Bretherton*, 1967]. Although a critical level will fully prevent a wave from propagating vertically, small Doppler frequency shifts may work either in the wave's favor, by helping it to reach higher altitudes, or against it, resulting in premature ducting or reflection. Winds do not preclude or severely hinder the phenomena we are considering. Winds orthogonal to the direction of GW propagation will not result in premature reflection or dissipation, consistent, for example, with predominantly zonal winds and northward/southward directionality of GWs observed during summer and winter time periods by *Hecht et al.* [2001].

5. Conclusions

[21] Thunderstorms typically excite GWs with periods near the local Brunt-Väisälä period of $\tau \simeq 10$ minutes [*Pierce and Coroniti*, 1966]. Many of these waves will break as they propagate upwards through the atmosphere. Waves breaking at mesopause heights may be able to excite propagating short-period ($\tau \simeq 5$ minutes) secondary waves that would be trapped in the upper mesosphere and lower thermosphere due to the local maximum of Brunt-Väisälä frequency. These waves would be thermally-ducted.

[22] In this paper the trapping of secondary waves at mesopause altitudes has been demonstrated through numerical simulation in a realistic atmosphere, with sources that approximate convective oscillations associated with thunderstorms. GWs with periods near 10 min were excited by a tropospheric oscillator; these waves propagated to mesopause heights where they broke and excited new, propagating, GWs with periods near 5 min, which then became trapped in the lower thermospheric duct. It can thus be concluded that breaking of tropospherically-generated GWs may be responsible for the excitation of short-period, thermally ducted modes in the upper mesosphere and lower thermosphere, which are frequently observed during airglow imaging experiments.

[23] **Acknowledgments.** We would like to thank Mike Taylor for his helpful advice. This research was supported by the National Science Foundation under grant ATM-01-23020 to the Pennsylvania State University.

References

Alexander, M. J., J. R. Holton, and D. R. Durran, The gravity wave response above deep tropical convection in a squall line simulation, *J. Atmos. Sci.*, *52*(12), 2212–2226, 1995.

Booker, J. R., and F. P. Bretherton, The critical layer for internal gravity waves in a shear flow, *J. Fluid Mech.*, *27*, 513–539, 1967.

Dewan, E. M., R. H. Picard, R. R. O'Neil, H. A. Gardiner, J. Gibson, J. D. Mill, E. Richards, M. Kendra, and W. O. Gallery, MSX satellite observations of thunderstorm-generated gravity waves in the mid-wave infrared images of the upper stratosphere, *Geophys. Res. Lett.*, *25*(7), 939–942, 1998.

Fovell, R., D. Durran, and J. R. Holton, Numerical simulation of convectively generated stratospheric gravity waves, *J. Atmos. Sci.*, *49*(16), 1427–1443, 1992.

Franke, P. M., and W. A. Robinson, Nonlinear behavior in the propagation of atmospheric gravity waves, *J. Atmos. Sci.*, *56*, 3010–3027, 1999.

Fritts, D. C., and L. Yuan, An analysis of gravity wave ducting in the atmosphere: Eckart's resonances in thermal and doppler ducts, *J. Geophys. Res.*, *94*(D15), 18,455–18,466, 1989.

Fritts, D. C., J. R. Isler, J. H. Hecht, R. L. Walterscheid, and O. Andreassen, Wave breaking signatures in sodium densities and OH nightglow 2. Simulation of wave and instability structures, *J. Geophys. Res.*, *102*(D6), 6669–6684, 1997.

Hecht, J. H., R. L. Walterscheid, D. C. Fritts, J. R. Isler, D. Senft, C. Gardner, and S. Franke, Wave breaking signatures in sodium densities and OH nightglow 1. airglow imaging, Na lidar, and MF radar observations, *J. Geophys. Res.*, *102*(D6), 6655–6668, 1997.

Hecht, J. H., R. L. Walterscheid, M. P. Hickey, and S. J. Franke, Climatology and modelling of quasi-monochromatic atmospheric gravity waves observed over Urbana, Illinois, *J. Geophys. Res.*, *106*(D6), 5181–5195, 2001.

Hedin, A. E., Extension of the MSIS thermospheric model into the middle and lower atmosphere, *J. Geophys. Res.*, *96*, 1159, 1991.

Horinouchi, T., T. Nakamura, and J. Kosaka, Convectively generated mesoscale gravity waves simulated throughout the middle atmosphere, *Geophys. Res. Lett.*, *29*(21), doi:10.1029/2002GL016069, 2002.

Larsen, M. F., W. E. Swartz, and R. F. Woodman, Gravity-wave generation by thunderstorms observed with a vertically-pointing 430 MHz radar, *Geophys. Res. Lett.*, *9*(5), 571–574, 1982.

LeVeque, R. J., Wave propagation algorithms for multidimensional hyperbolic systems, *J. Comp. Phys.*, *131*, 327–353, 1997.

LeVeque, R. J., *Finite Volume Methods for Hyperbolic Problems*, Cambridge University Press, 2002.

Piani, C., D. Durran, M. J. Alexander, and J. R. Holton, A numerical study of three-dimensional gravity waves triggered by deep tropical convection and their role in the dynamics of the QBO, *J. Atmos. Sci.*, *57*(22), 3689–3702, 2000.

Pierce, A. D., and S. C. Coroniti, A mechanism for the generation of acoustic-gravity waves during thunderstorm formation, *Nature*, *210*(5042), 1209–1210, 1966.

Sentman, D. D., E. M. Wescott, R. H. Picard, J. R. Winick, H. C. Stenbaek-Nielsen, E. M. Dewan, D. R. Moudry, F. T. São Sabbas, M. J. Heavner, and J. Morrill, Simultaneous observations of mesospheric gravity waves and sprites generated by a midwestern thunderstorm, *J. Atmos. Solar-Terr. Phys.*, *65*, 537–550, 2003.

Stull, R. B., Internal gravity waves generated by penetrative convection, *J. Atmos. Sci.*, *33*, 1279–1286, 1976.

Taylor, M. J., and H. A. Hapgood, Identification of a thunderstorm as a source of short period gravity waves in the upper atmospheric nightglow emissions, *Planet. Space Sci.*, *36*, 975–985, 1988.

Taylor, M. J., D. N. Turnbull, and R. P. Lowe, Spectrometric and imaging measurements of a spectacular gravity wave event observed during the ALOHA-93 campaign, *Geophys. Res. Lett.*, *22*(20), 2849–2852, 1995.

Vadas, S. L., D. C. Fritts, and M. J. Alexander, Mechanism for the generation of secondary waves in wave breaking regions, *J. Atmos. Sci.*, *60*, 194–214, 2003.

Walterscheid, R. L., J. H. Hecht, R. A. Vincent, I. M. Reid, J. Woithe, and M. P. Hickey, Analysis and interpretation of airglow and radar observations of quasi-monochromatic gravity waves in the upper mesosphere and lower thermosphere over Adelaide, Australia, *J. Atmos. Solar-Terr. Phys.*, *61*, 461–478, 1999.

Walterscheid, R. L., G. Schubert, and D. G. Brinkman, Small-scale gravity waves in the upper mesosphere and lower thermosphere generated by deep tropical convection, *J. Geophys. Res.*, *106*(D23), 31,825–31,832, 2001.

Yamada, Y., H. Fukunishi, T. Nakamura, and T. Tsuda, Breaking of small-scale gravity waves and transition to turbulence observed in OH airglow, *Geophys. Res. Lett.*, *28*(11), 2153–2156, 2001.

Zhou, X., J. R. Holton, and G. L. Mullendore, Forcing of secondary waves by breaking of gravity waves in the mesosphere, *J. Geophys. Res.*, *107*(D7), doi:10.1029/2001JD001204, 2002.

J. B. Snively and V. P. Pasko, CSSL Laboratory, Department of Electrical Engineering, The Pennsylvania State University, 211B Electrical Engineering East, University Park, PA 16802, USA. (jbs231@psu.edu; vpasko@psu.edu)